Published in final edited form as:

Mol Cancer Res. 2015 June ; 13(6): 982–992. doi:10.1158/1541-7786.MCR-14-0660-T.

EphB1 Suppression in Acute Myelogenous Leukemia: Regulating the DNA Damage Control System

K.R. Kampen[1], **F.J.G. Scherpen**[1], **G. Garcia-Manero**[2], **H. Yang**[2], **G.J.L. Kaspers**[3], **J. Cloos**[3], **C.M. Zwaan**[4], **M.M. van den Heuvel-Eibrink**[4], **S.M. Kornblau**[2], and **E.S.J.M. De Bont**[1]

[1]Department of Pediatric Oncology, Beatrix Children's Hospital, University Medical Center Groningen, University of Groningen,Groningen, the Netherlands. [2]Department of Leukemia, The University of Texas MD Anderson Cancer Center, Houston, Texas. [3]Department of Pediatric Oncology, VU University Medical Center, Amsterdam, the Netherlands. [4]Department of Pediatric Oncology, Erasmus MC-Sophia Children's Hospital, Rotterdam, the Netherlands.

Abstract

Loss of ephrin receptor (EphB1) expression may associate with aggressive cancer phenotypes; however, the mechanism of action remains unclear. To gain detailed insight into EphB1 function in acute myelogenous leukemia (AML), comprehensive analysis of EphB1 transcriptional regulation was conducted. In AML cells, EphB1 transcript was inversely correlated with EphB1 promoter methylation. The presence of EphB1 allowed EfnB1 ligand–mediated p53 DNA binding, leading to restoration of the DNA damage response (DDR) cascade by the activation of ATR, Chk1, p53, p21, p38, CDK1^{tyr15}, and Bax, and downregulation of HSP27 and Bcl2. Comparatively, reintroduction of EphB1 expression in EphB1-methylated AML cells enhanced the same cascade of ATR, Chk1, p21, and CDK1^{tyr15}, which consequently enforced programmed cell death. Interestingly, in pediatric AML samples, EphB1 peptide phosphorylation and mRNA expression were actively suppressed as compared with normal bone marrow, and a significant percentage of the primary AML specimens had EphB1 promoter hyper-methylation. Finally, EphB1 repression

Corresponding Author: E.S.J.M. de Bont, Beatrix Children's Hospital, University Medical Center Groningen, University of Groningen PO Box 30.001, 9700 RB Groningen, the Netherlands. Phone: 00-315-0361-4146; Fax: 00-315-0361-1671; e.s.j.m.de.bont@umcg.nl.

Authors' Contributions

Conception and design: K.R. Kampen, E.S.J.M. De Bont

Development of methodology: K.R. Kampen, G. Garcia-Manero, E.S.J.M. De Bont

Acquisition of data (provided animals, acquired and managed patients, provided facilities, etc.): G. Garcia-Manero, G.J.L. Kaspers, C.M. Zwaan, M.M. van den Heuvel-Eibrink, J. Cloos, S.M. Kornblau, E.S.J.M. De Bont

Analysis and interpretation of data (e.g., statistical analysis, biostatistics, computational analysis): K.R. Kampen, G. Garcia-Manero, S.M. Kornblau, E.S.J.M. De Bont

Writing, review, and/or revision of the manuscript: K.R. Kampen, F.J.G. Scherpen, H. Yang, G.J.L. Kaspers, M.M. van den Heuvel-Eibrink, G. García-Manero, C.M. Zwaan, J. Cloos, S.M. Kornblau, E.S.J.M. De Bont

Administrative, technical, or material support (i.e., reporting or organizing data, constructing databases): K.R. Kampen, F.J.G. Scherpen, H. Yang, G.J.L. Kaspers, M.M. van den Heuvel-Eibrink, G. Garcia-Manero, C.M. Zwaan, J. Cloos, S.M. Kornblau, E.S.J.M. De Bont

Study supervision: E.S.J.M. De Bont

Supplementary data for this article are available at Molecular Cancer Research Online (http://mcr.aacrjournals.org/).

Disclosure of Potential Conflicts of Interest

No potential conflicts of interest were disclosed.

associated with a poor overall survival in pediatric AML. Combined, the contribution of EphB1 to the DDR system reveals a tumor-suppressor function for EphB1 in pediatric AML.

Implications—The tumor-suppressor function of EphB1 is clinically relevant across many malignancies, suggesting that EphB1 is an important regulator of common cancer cell trans forming pathways.

Introduction

Ephrin tyrosine kinase receptors take part in the largest family of receptor tyrosine kinases, consisting of cell surface membrane bound kinases that include at least 14 receptors and 8 ligands. The most extensively investigated functions of ephrin receptors and ligands involve cell adhesion and migration via bidirectional signaling. Eph receptors are known for their contradictory function to promote or suppress cancer progression depending on their cellular contexts. EphA1/2/4/5/7 and EphB2/4 receptor overexpression has been shown to contribute to the pathogenesis of tumors with respect to tumor growth, tumor grade, and patient outcome in hepatocellular carcinoma, pancreatic adenocarcinoma, astrocytoma, and gliomas (1–5). In contrast, Eph receptors can also fulfill tumor-suppressor functions. EphA2 receptor activation has been implicated to function as a tumor suppressor in breast cancer, non–small cell lung carcinoma and prostate cancer cells (6–9). Ephrin-A1 induced activation of EphA2 in breast cancer cells was shown to decrease *in vivo* tumorigenicity in mouse models (10, 11). Loss of EphB1 has previously been shown to associate with an aggressive cancer phenotype in gastric carcinoma and serous ovarian cancers (12, 13). Various mechanisms are described to suppress EphR expression in cancer pathogenesis; transcriptional repression of *EphB2* by *c-REL*, frequent deletion of the chromosomal region 1p36 encounters *EphA2*, *EphA8*, and *EphB2* loss in many cancers, or hypermethylation of the CpG Island on the promoter regions resulting in loss of function of *EphB6* in breast cancer, *EphB2* in colorectal cancer and *EphA7* in prostate cancer (10, 11, 14–18). In EfnB1 Lck-Cre KO mice, it has been shown that Efn ligands are redundant in expression and functionality in relation to normal lymphoid hematopoiesis (19). In contrast, in acute lymphoid leukemia (ALL), the number of epigenetic-inactivated Eph receptors and ligands was associated with a shortened overall survival (OS; ref. 20). In focus of *EphB4* hypermethylation, reexpression of EphB4 by constitutive overexpression in an ALL cell line reduced the leukemic cell proliferation and increased apoptosis. Data on mechanistic consequences related to Eph receptor loss of function are scarce. In this study, we aimed to gain detailed biologic insight into the Eph receptor signaling in acute myelogenous leukemia (AML).

In this study, we explored the expression of *Eph* receptors and found a common downregulation of *EphB1* assigned to promoter hypermethylation. Interestingly, biologic insights revealed a tumor-suppressor function for EphB1 in AML by coordinating the DNA damage response (DDR) system. Rein-troduction of EphB1 blocked AML cell-cycle progression and activated programmed cell death pathways. Clinical consequence of EphB1 suppression in AML was manifested in its association with a longer time to reach a complete remission and a poorer OS.

Materials and Methods

Patient samples and AML cell lines

After getting written informed consent, the mononuclear cell fraction (MNC) of bone marrow form healthy controls (NBM, normal bone marrow) and pediatric AML patients was obtained and cryopreserved, approved by the Medical Ethical Committee of the University Medical Center Groningen METC 2010.036 and 2013.281. The cryopreserved bone marrow cells were thawed rapidly at 37°C and diluted in a 6 mL volume of newborn calf serum, as described previously (21).

The cell lines HL60, THP-1, HEL, NB4, and MOLM13 were obtained from the ATCC, cultured in RPMI-1640 medium (Lonza) supplemented with 1% penicillin–streptomycin (Life Technologies Europe BV) and 10% FCS (Bodinco). AML patients' samples and AML cell lines all showed severe DNA damage by pH2AX and not in pediatric NBM (Supplementary Fig. S1A).

Compounds

EfnB1 ligand was used in culture to stimulate EphB1 receptor on AML cells (1 μg/mL recombinant mouse Ephrin B1 ligand, Fc Chimera; R&D Systems). 5-Aza-2′-deoxycytidine (200 nmol/L; Sigma Aldrich) was used as a demethylating agent. Control Fc chimeric protein did not show relevant *in vitro* effects (data not shown). Etoposide (20 mg/mL stock) was used at a concentration of 0.5 mg/mL as a genotoxic agent.

Fluorescence-activated cell sorting

Cells were blocked by PBS 1% BSA (Sigma Aldrich), and stained with EphB1 antibody (Clone 88512; R&D systems) or CD34-PE and CD38-PerCP-Cy5.5 antibodies (BD Biosciences). Primary EphB1 antibodies were visualized using a Rabbit anti-Mouse PE-conjugated secondary antibody (Dako cytomation). For apoptosis analysis, the AML cells were stained with 100 μL of Annexin V/propidium iodide (PI) solution (1 mL staining buffer, with the addition of 20 μL Annexin V–FITC/PE, and 20 μL PI; Roche). For cell-cycle analysis cells, we fixed in methanol, blocked and incubated with 2 μL phospho-Histone H3 antibody (Cell Signaling Technology) for 20 minutes, washed and stained with 2 μL PI. For proliferation analysis, cells were incubated with BrdUrd (5-bromo-2′-deoxyuridine) for 4 hours after which the cells were fixed, denaturated, and stained for anti-BrdUrd that was visualized with a Rabbit anti-Mouse FITC–conjugated secondary antibody (Dako cytomation). AML cells were analyzed using LSRII (BD FACS DIVA software; BD Biosciences).

ADAM17 ELISA

The human ADAM17/TACE duoset was used to determine ADAM17 shedding involvement in EphB1 cleavage in THP-1 cells. THP-1 cells (1×10^6) were left for 24 hours either untreated or EfnB1 treated. Cells were collected in cell lysis buffer (Cell Signaling Technology) supplemented with 1 mmol/L phenyl-methylsulfonylfluoride (Sigma Aldrich) and analyzed for ADAM17 protein expression according to the manufacturer's protocol (R&D systems).

Western blot analysis

A total of 1 to 2 × 10^6 HL-60, THP-1, and MOLM13 cells were lysed in laemmli sample buffer (Bio-Rad laboratories). Proteins were separated by SDSPAGE, and transported to nitrocellulose membranes. The membranes were incubated overnight with monoclonal primary antibodies for pATR, pCDK1 (Tyr15), CDK1, CyclinB1, pChk1, pChk2, p21 (Cell Signaling Technology), Bcl-2, Bax (CalBiochem; Merck), EphB1 and actin (Santa Cruz Biotechnology), and p53 (PAb240 from Abcam) and for 1 hour with horseradish peroxidase–conjugated secondary antibodies (DAKO cytomation). Protein bands were visualized by chemiluminescence, on an X-ray film.

Human phospho-kinase antibody array

Human Phospho-Kinase Antibody Array kits were used from R&D Systems to measure protein phosphorylation (46 phosphor-ylation sites corresponding to 36 proteins) according to the manufacturer's protocol. The protein spots are visualized by chemiluminescence, on an X-ray film, and scanned. Signaling intensity of the proteins was analyzed with array software and processed as described previously (ScanAlyze; Eisen Software, http://rana.lbl.gov/eisen; ref. 22).

Quantitative real-time PCR

EphB1, p21, Bcl-2, and *p53* mRNA expression levels were analyzed using SYBR Green quantitative real-time PCR (qRT-PCR; Applied Biosystems Applera) with *HPRT* as a reference gene. Complementary DNA synthesis was accomplished from 1 μg RNA (RNeasy mini kit; Qiagen). Relative mRNA expression levels of the gene of interest were calculated using the $\Delta\Delta C_t$ method relatively to the mean *HPRT* mRNA expression levels. Primer sequences are depicted in Supplementary Table S1.

Cloning retroviral vectors

Retroviral supernatants were generated by cotransfection *pMSCV–iGFP* constructs, or empty vector *pMSCV-iGFP*, and packaging plasmid pCLampho into 293T cells by using FuGENE HD transfection reagent (Roche). Transduction efficiency was measured by FACS analysis (Supplementary Fig. S1C and S2C).

DNA bisulfite treatment and methylation analysis

DNA was isolated according to the manufacturers' (Qiagen; DNA mini kit) protocol. DNA was modified with sodium bisulfite. Bisulfite pyrosequencing and bisulfite sequencing was performed as described previously (20). DNA methylation density ranged from 5% to 96% for AML cell lines and 1% to 35% for primary AML ($n = 21$) and NBM ($n = 5$) samples. Primer sequences are included in Supplementary Table S1.

Gene-expression data analysis

The Dutch Childhood Oncology Group (DCOG) pediatric AML cohort gene-expression array dataset was used for analyzing EphB1 expression in relation to clinical parameters. Details on gene-expression array analysis and the AML patient samples were previously described (GSE22056ID: 200022056; ref. 23). Data for the time to reach a complete

remission were available of 79 patient samples. For the OS, we examined EphB1 (210753_s_at probe with highest coverage of the most unique EphB1 region) gene-expression data of 100 pediatric AML samples. The mean EphB1 expression (log_2 of 4.59) was used as a cutoff point for the Kaplan–Meier analysis resulting in groups of 42 patients with low EphB1 expression and 58 patients with high EphB1 expression.

Validation dataset came from the St. Jude Children's Research Hospital that can be downloaded from the website; http://www.stjuderesearch.org/site/data/AML1 (24). This dataset contains gene-expression data of 97 pediatric AML patient samples divided into t(8;21), INV(16), 11q23, M7, and other cytogenetic subgroups pediatric AMLswith corresponding relapsedata.Probe 210753_s_at expression (highest coverage of most unique EphB1 gene region) was log_2 transformed to determine differences between favorable and unfavorable cytogenetic subgroups. Favorable cytogenetic subgroups; $n = 21$ for t(8;21) and $n = 14$ for INV(16), and unfavorable; $n = 23$ for 11q23 and $n = 10$ for M7 pediatric AMLs.

Chromatin immunoprecipitation

A total of 12.5×10^6 treated and untreated THP-1 cells were fixed in 1% formaldehyde for 10 minutes after which glycine (1:20, 2.5 mol/L; Sigma Aldrich) was added. After a three-step cell lysis the cells were sonificated for 10 cycles of 20 seconds. Chromatin immunoprecipitation (ChIP) was performed by dissolving the nuclei pellets in 110 μL Chip Buffer (ChIP-IT Express Chromatin Immunoprecipitation Kit, Active Motif) with protease inhibitors, putting aside 10 μL input DNA. Lysates were incubated with 2 μg p53 antibodies (PAb1620 or PAb240 from Abcam) for 4 hours, thereafter, adding 60 μL Dynabeads (Life Technologies). After reverse cross-linking DNA was purified from IP samples and input DNA according to the manufacturer's protocol (PCR puri-fication kit; Qiagen).

Cell survival assays

Quantification of leukemia cell viability was carried out using WST-1 assays for AML cell lines. WST-1 assays were performed in triplicates according to the manufacturer's protocol (Roche). Cells were seeded at a density of 1×10^5 cells per 100 μL/well. Mitochondrial activity of AML cell was measured after 48 hours using a microplate reader at 450 nm (Benchmark; Bio-Rad Laboratories). Cell survival percentages are determined relative to untreated cells.

Statistical analysis

Mean and SDs of at least three independent evaluations are represented. Statistical package for the social science (SPSS 17) software was used for graphing box-plots. Significant correlations were determined using a Pearson correlation coefficient (Fig. 1A). The Mann–Whitney *U* tests were used to determine significant differences between two individual patient groups (as indicated). The Kruskall–Wallis test was used to examine differences between more than two patient groups for significance (as indicated). Unpaired two-tailed Student *t* tests were used for all *in vitro* cell line analysis comparing two conditional experimental groups in at least triplicates. The paired samples *t* test was used for determining the overall effect of *EphB1* overexpression in AML cell lines and primary AML

samples. The Kaplan–Meier analysis was used for defining the cumulative survival based upon high or low EphB1 expression.

Results

EphB1 suppression in AML; a role for DNA methylation

Common genetic deregulation of EphR in cancer pathogenesis urged us to determine the different levels of EphR transcriptional regulation in various AML cell lines. We examined a panel of AML cell lines for their EphA and EphB receptor and EfnB ligand mRNA expression levels in comparison with their promoter methylation density (the percentage of CpG sites methylated for the particular gene promoter) using quantitative RT-PCR and bisulfite pyrosequencing, respectively (Fig. 1A). Interestingly, among EphA and EphB receptors, the promoter of *EphB1* was frequently methylated and presented a unique significant inverse correlation between *EphB1* mRNA expression levels and promoter methylation (Pearson correlations; $P = 0.717$ for EphA2, $P = 0.841$ for EphA4, $P = 0.301$ for EphA6, $P = 0.256$ for EphA7, $P = 0.010$ for *EphB1*, $P = 0.116$ for *EphB2*, $P = 0.153$ for *EphB3*, $P = 0.198$ for *EphB4*, $P = 0.094$ for *EphB6*, $P = 0.469$ for *EfnB1*, and $P = 0.544$ for *EfnB2*)

EfnB1 mediated growth inhibition and apoptosis of EphB1-expressing AML cells

To gain mechanistic insights into the suppressive role of the EphB1 forward signaling in AML, we investigated the influence of EfnB1 stimulation on AML cell proliferation and survival in AML cell line models. First, we examined EphB1 membrane protein expression in AML cell lines. Approximately 70% of the THP-1 cells express EphB1 on their cell surface ($EphB1^{high}$), only 25% to 30% 30% of the HL60 and 10% of the MOLM-13 cells ($EphB1^{low}$, Fig. 1B). EfnB1 stimulation of AML cell lines demonstrated to inhibit the leukemic growth by 50% in $EphB1^{high}$ THP-1 cells as compared with untreated controls (Fig. 1C, Student *t* test, $P = 0.001$), but not in $EphB1^{low}$ HL60 and MOLM-13 cells. Next, we examined the effect of EfnB1 stimulation on AML cell survival by Annexin V/PI flow cytometric analysis. EfnB1 stimulation induced programmed cell death by 25% in THP-1 as compared with the untreated controls (Fig. 1D). Long-term stimulation with a single dose of EfnB1 reduced the THP-1 AML cell survival by 75% at day 9 (Fig. 1E, Student *t* test, $P = 0.029$). To measure EfnB1–EphB1 complex induced cleavage of the receptor in AML cells, we determined ADAM17 metalloprotease expression. Determination of ADAM17 revealed that EfnB1 stimulation increased ADAM17 protein expression in THP-1 cells, suggestive for induced EphB1 cleavage (Fig. 1F, Student *t* test, $P = 0.015$).

EfnB1 induced G_2–M cell-cycle arrest of EphB1-expressing AML cells

We hypothesized that the phenotypic effects of growth inhibition and the induction of apoptosis could be assigned to a defect in cell-cycle regulation. Cell-cycle analysis upon EfnB1 ligand stimulation of $EphB1^{high}$ cells revealed an increase in the number of cells in G_2–M phase of the cell cycle after which these cells were prone to go into apoptosis (Fig. 2A, paired samples *t* test, $P = 0.028$). Here, we show that the number of phospho-histone H3–expressing mitotic cells decreased by 40% upon EfnB1 treatment in THP-1 (Fig. 2B). In line with these findings, we observed a 25% reduction in the amount of proliferating cells

after 48 hours EfnB1 treatment and 4 hours of BrdUrd incorporation (Fig. 2B). Confirming the induction of apoptosis, immunoblot analysis showed a downregulation of antiapoptotic Bcl-2 and an induction of proapoptotic $Bax_{\alpha/\beta}$ (Fig. 2C). Simultaneously, the phosphorylation of the inactivating CDK1 (CDC2) Tyr15-site was upregulated in EfnB1-stimulated THP-1 cells, which might be initiated by the increased total CDK1 protein levels that we found (Fig. 2C). In addition, CyclinB1 protein expression was enhanced in EfnB1 treated THP-1 cells. Phospho-proteome analysis of untreated and EfnB1-stimulated THP-1 cells unraveled downstream machinery that contributed to the G_2–M cell-cycle arrest (Fig. 2D). As expected, the phosphorylation of cell-cycle regulators p27, p38 and p53 was increased upon EfnB1 stimulation of $EphB1^{high}$ AML cells. Moreover, to gain more insights into the observed G_2–M cell-cycle arrest, we found increased ATR, Chk1, and p38 phosphorylation and p53 total protein expression by EfnB1 stimulation of THP-1 cells, whereas phosphorylation of Chk2 remained largely unchanged (Fig. 2E). Moreover, Src phosphorylation showed to be decreased by EfnB1 treatment in THP-1 cells. In accordance with proteomics, quantitative RT-PCR analysis showed that the expression of *p53* was increased together with downstream cell-cycle inhibitor *p21* (Fig. 2F, Student *t* test, both *p21* and *p53* $P < 0.001$). ChIP of p53 followed by quantitative RTPCR analysis of p53 distal binding sites on *p21* and *MDM2* revealed that EfnB1 stimulation of THP-1 cells significantly increased the p53 DNA binding capacity (Fig. 2G, Student *t* test, both *p21* and *MDM2* $P < 0.001$). EfnB1 induced cell cycle inhibitory effects were not observed in $EphB1^{low}$ HL60 AML cells (Supplementary Fig. S1B). These data implicate that EfnB1 can induce a G_2–M cell-cycle arrest in $EphB1^{high}$ AML cells by enhancing p53 DNA binding that prevents the AML cells from entering mitosis and finally results in apoptosis. The restoration of the DDR system upon EfnB1 treatment can only occur in the presence of DNA damage. Therefore, we analyzed phoshorylated γH2AX levels in the AML. Apparent DNA damage could be observed in AML cell lines and pediatric AML patients samples, but not in the NBM control (Fig. 2H). Moreover, EfnB1 stimulation was shown to significantly induce cellular sensitivity to the genotoxic agent etoposide in THP-1 (Fig. 2I, Student *t* test, EfnB1 reduced cell survival; *, $P < 0.001$).

Programmed cell death as a consequence of EphB1 reintroduction in *EphB1* methylated AML cell lines

Using 5-Aza-2′-deoxycytidine as demethylation treatment in *EphB1*-methylated HL60 AML cells, we found an increase in EphB1 protein expression by flow cytometry, suggestive for reversible *EphB1* promoter demethylation (Fig. 3A, Student *t* test, $P < 0.001$). To specifically determine whether the EphB1 receptor was indeed the main mediator of the EfnB1 induced cell-cycle arrest, we introduced *EphB1* overexpression DNA constructs in the *EphB1* hypermethylated AML cell lines HL60 (*p53*-null) and MOLM13 (*p53*-wildtype), using a constitutive promoter in front of the *EphB1* gene to induce constitutive transcription. An empty vector control was used as reference. Reintroduction of constitutive *EphB1* mRNA expression increased *EphB1* transcription by more than 1,000-fold in both AML cell lines (Fig. 3B, Student *t* test, $P < 0.001$ for HL60 and MOLM13). Flow cytometric analysis showed an induction in EphB1 membrane expression in both AML cell lines (Fig. 3B). Western blot analysis confirmed the induction of EphB1 protein expression in EphB1 overexpression AML cell lines (Fig. 3B). Cell-cycle progression by BrdUrd incorporation

showed a decreased percentage of proliferating AML cells in EphB1 overexpression MOLM13 cells (Fig. 3C). Reintroduction of *EphB1* into HL60 and MOLM13 cells presented a distinct phenotype, characterized by an increase in apoptosis solely of the *EphB1* transduced populations relatively to *empty vector* control cells (Fig. 3D, Supplementary Fig. S1C, Student *t* test, MOLM13 $P < 0.001$). Next, we showed that the remaining viable *EphB1*-overexpressing cells were increasingly susceptible to EfnB1 ligand–induced apoptosis as compared with empty vector controls in both AML cell lines (additional 20%–40% increase in apoptosis, Fig. 3D). Reexpression and subsequent stimulation of the EfnB1/EphB1 forward signaling in *EphB1*-methylated AML cells markedly decreased the AML cell survival in two independent cell lines (Supplementary Fig. S1D, paired samples *t* test, $P = 0.040$, overall apoptosis induction 16% ± 12% empty vector and 44% ± 18% in *EphB1* overexpression cells). Moreover, similar as was observed in THP-1, EphB1 overexpression MOLM13 and HL60 cells were significantly more sensitive to genotoxicity induced by 48 hours etoposide treatment (Fig. 3E, Student *t* test, $P < 0.001$). Relative mRNA expression of Bcl-2 was decreased in both *EphB1*-overexpressing HL60 and MOLM13 cells (Fig. 3F, Student *t* test, $P = 0.014$ and $P = 0.037$). Increased *p53* transcription was evident in *EphB1*-overexpressing MOLM13 cells, but not in HL60 *p53*-null cells (Student *t* test, $P = 0.038$). Immunoblot analysis revealed p53-independent regulation of enhanced levels p21 protein expression upon activation of the ATR–Chk1 axis in HL60 *p53*-null cells (Fig. 3G). Phosphorylation of downstream $CDK1^{tyr15}$ was enhanced in both HL60 and MOLM13 *EphB1* overexpression cells compared with the empty vector control cells (Fig. 3G).

EphB1 suppression associated with unfavorable cytogenetics, relapses and decreased probability of OS in pediatric AML; a role for *EphB1* methylation

To evaluate whether our proposed model also persists in primary pediatric AML, we extended our analysis from previous study by including NBM controls from the high-throughput kinase activity arrays (25). We showed that kinase activity of the EphB1 peptide was significantly lower in pediatric AML sample lysates as compared with NBM lysates (Fig. 4A and Supplementary Fig. S2A, Mann–Whitney *U* test, $P = 0.022$). Next, we analyzed *EphB1* mRNA expression levels in a cohort of pediatric AML patient samples ($n = 27$) and NBM controls ($n = 8$). *EphB1* mRNA expression was found to be significantly reduced in AML as compared with NBM (Mann–Whitney *U* test, $P = 0.030$). Interestingly, AML samples from patients with cytogenetically unfavorable prognosis showed significantly lowest *EphB1* mRNA expression, followed by samples from patients with other karyo-type, whereas NBM controls presented highest *EphB1* mRNA expression levels (Fig. 4B, Kruskal–Wallis test, $P = 0.013$). Validation in a publicly available gene-expression dataset of an independent pediatric AML cohort confirmed that *EphB1* expression was significantly lower in cytogenetically unfavorable pediatric AML as compared with favorable AML (Supplementary Fig. S2B, Mann–Whitney *U* test, $P = 0.008$). Bisulfate pyrosequencing revealed increased methylation of the *EphB1* promoter as compared with NBM in 4 of 21 AML samples. Hypermethylation of the *EphB1* promoter was primarily found in unfavorable AML patient samples (Kruskal–Wallis test, Fig. 4B, $P = 0.103$). Using the DCOG pediatric AML gene-expression dataset, we found that *EphB1* expression was significantly adversely correlated with the time to reach a complete remission (Fig. 4C,

Pearson correlation, $P = 0.041$). Interestingly, therapy-resistant AML patient samples expressed lower levels of *EphB1* compared with therapy responders (Mann–Whitney U test, $P = 0.026$). Interestingly, the OS was associated with *EphB1* expression (Pearson correlation, $P = 0.008$). Pediatric AML patients with low *EphB1* expression showed a significantly reduced OS (Fig. 4D, Kaplan–Meier, $P = 0.043$).

We challenged to transduce two independent EphB1^{low} primary pediatric AML patient samples with our established *EphB1* overexpression construct and the empty vector controls. Patient AML1 showed a lack of EphB1 expression and high CD34 (~70%) and CD38 (~70%) expression levels by flow cytometry (Fig. 4E and Supplementary Fig. S2C). Patient AML2 presented low EphB1 (~27%) and CD34 (~30%) expression levels and high CD38 (~85%) expression levels. Transduction efficiencies were approximately 35% in AML1 and 75% to 90% in AML2 (Fig. 4F and Supplementary Fig. S2C). EphB1 overexpression increased membrane protein expression levels by >50% (Fig. 4G and Supplementary Fig. S2C). In both AML samples, we found that EphB1 overexpression reduced the AML cell counts by 20%±3.5% at day 7 after transduction (Fig. 4H, paired samples t test, $P = 0.016$, cell counts $1.45 \times 10^6 \pm 9 \times 10^5$ in empty vector controls and $1.16 \times 10^6 \pm 7 \times 10^5$ in *EphB1*-overexpressing AML cells, SEM 3.6×10^5 and 2.9×10^5). These findings may suggest a tumor suppressor function for EphB1 in primary pediatric AML.

Discussion

Here, we describe that *EphB1* was commonly suppressed in pediatric AML. When EphB1 is present, ligand activation restored the downstream DDR system (p53/p21/Bcl-2) through Chk1 phosphorylation–mediated repression of G_2–M transition via CDK1^{tyr15}. *EphB1* reintroduction in EphB1 methylated AML cells operates through similar pathways for cell-cycle repression in AML, which allows *p53*-independent routes. The clinical impact of *EphB1* suppression in pediatric AML is illustrated by the enhanced time to reach a complete remission and the association with a reduced OS. *EphB1* promoter methylation affected 20% of the pediatric AML samples. These findings emphasize the importance of EphB1 functioning as a tumor suppressor in AML.

A previous study revealed that restoration of ligand-induced EphB4-regulated pathways in breast cancer biology is responsible for antioncogenic effects *in vitro* and *in vivo* (26). Here, we defined the antioncogenic effects of *EphB1* reintroduction and ligand stimulatory effects on p53, Chk1, p21, CDK1, Bcl-2, and BAX as important regulatory proteins for downstream EphB1 signaling in AML. The increase in p21 was previously shown to be critical for nuclear retention of the CDK1–CyclinB1 complex by sustained phosphorylation of CDK1^{tyr15} (27). Among the affected pathways are important DDR proteins that facilitate an “anticancer barrier” of normal functioning cells to get rid of or repair DNA damaged cells. The DDR system was found to be commonly defective in AML (28). DNA damage was defined by increased levels of γ-2HAX and phosphorylated ATM in bone marrow biopsies of AML patients that correlated with blast percentages. These proteins were not expressed in healthy bone marrow biopsies. The investigators suggested that AML cells are defective in their DDR system due to inactivation of checkpoint kinases-1/2, which is in accordance with the paradigm established for solid tumors (29). In this study, we found that reintroduction of

EphB1 expression and ligand-induced stimulatory signals partly restores the DNA damage control system via Chk1, which forced the AML cells in an G_2–M cell-cycle arrest. The phenotype of *EphB1* reintroduction was more apparent in AML cell lines compared with primary AML blasts, probably due to the fact that in general cell lines are increasingly DNA damaged during their passages, and their proliferation rate is higher compared with the primary blasts. The fact that HL60 *p53*-null cells are also vulnerable to *EphB1* reintroduction may imply that EphB1 can also function via *p53*-independent activation of the Chk1/p21 cascade for G_2–M suppression.

EphB1 expression is generally low in AML, which could only partially be explained by methylation in 20% of the AML patients. Another contributor may be chromosome 3 alterations in pediatric AML patients. *EphB1* is located on chromosome 3q21. This location is a fragile site region of chromosome 3, and is mainly known to be affected in therapy-related adult AML (30). Chromosome 3 aberrations are rare in pediatrics, but do occur as translocations, inversions and deletions (30, 31). These genetic alterations may contribute to aberrant expression of *EphB1* in AML patients. Moreover, there are other mechanisms that may interfere with *EphB1* expression. Overexpression of wild-type c-Cbl has been shown to enhance EphB1 ubiquitination and lysosomal degradation (32). This leaves the suggestion that c-Cbl overexpression may contribute to suppression of EphB1 expression and function. However, c-Cbl mutations do not frequently occur in pediatric AML (33). The tumor-suppressor function of EphB1 in AML and the association in a variety of cancers between loss of expression and aggressive tumor phenotypes implies that EphB1 is an important regulator of common cancer cell–transforming pathways (12, 13, 34). Conformingly, we used the MethHC DNA methylation database in human cancers (35) to analyze EphB1 promoter CpG site methylation and found common promoter hypermethylation enriched at the 5′ untranslated regions (Supplementary Fig. S3, all cancers $P < 0.005$). EphB1 promoter hypermethylation was significantly higher as compared with normal sample controls in many cancers, including breast, lung, cervical, colon, stomach, and prostate cancer. Similar to our NBM samples, the normal tissue sample controls showed no signs of methylation in the EhB1 promoter region.

In this study, we defined the biologic and clinical impact of EphB1 as a tumor suppressor in pediatric AML, which encourages further investigation on (epigenetic) mechanisms that regulate EphB1 expression and activation for the development of potential EphB1-inducing therapies.

Supplementary Material

Refer to Web version on PubMed Central for supplementary material.

Acknowledgments

The authors thank Marcel van Vugt for his expert opinion on DNA damage and cell-cycle pathways and the useful discussions. The authors thank the patients who donated leukemia specimens; physician assistants, nurse practitioners, and fellows who acquired specimens.

Grant Support

K.R. Kampen was supported by a grant from the Foundation for Pediatric Oncology Groningen, the Netherlands (SKOG). S.M. Kornblau was supported by a grant from the Leukemia and Lymphoma society.

The costs of publication of this article were defrayed in part by the payment of page charges. This article must therefore be hereby marked *advertisement* in accordance with 18 U.S.C. Section 1734 solely to indicate this fact.

References

1. Cui XD, Lee MJ, Yu GR, Kim IH, Yu HC, Song EY, et al. EFNA1 ligand and its receptor EphA2: potential biomarkers for hepatocellular carcinoma. Int J Cancer. 2010; 126:940–9. [PubMed: 19642143]
2. Giaginis C, Tsourouflis G, Zizi-Serbetzoglou A, Kouraklis G, Chatzopoulou E, Dimakopoulou K, et al. Clinical significance of ephrin (eph)-A1, -A2, -a4, -a5 and -a7 receptors in pancreatic ductal adenocarcinoma. Pathol Oncol Res. 2010; 16:267–76. [PubMed: 19949912]
3. Li X, Wang Y, Wang Y, Zhen H, Yang H, Fei Z, et al. Expression of EphA2 in human astrocytic tumors: correlation with pathologic grade, proliferation and apoptosis. Tumour Biol. 2007; 28:165–72. [PubMed: 17519535]
4. Lu Z, Zhang Y, Li Z, Yu S, Zhao G, Li M, et al. Overexpression of the B-type Eph and ephrin genes correlates with progression and pain in human pancreatic cancer. Oncol Lett. 2012; 3:1207–12. [PubMed: 22783419]
5. Tu Y, He S, Fu J, Li G, Xu R, Lu H, et al. Expression of EphrinB2 and EphB4 in glioma tissues correlated to the progression of glioma and the prognosis of glioblastoma patients. Clin Transl Oncol. 2012; 14:214–20. [PubMed: 22374425]
6. Foveau B, Boulay G, Pinte S, Van RC, Rood BR, Leprince D. The receptor tyrosine kinase EphA2 is a direct target gene of hypermethylated in cancer 1 (HIC1). J Biol Chem. 2012; 287:5366–78. [PubMed: 22184117]
7. Ishikawa M, Miyahara R, Sonobe M, Horiuchi M, Mennju T, Nakayama E, et al. Higher expression of EphA2 and ephrin-A1 is related to favorable clinicopathological features in pathological stage I non–small cell lung carcinoma. Lung Cancer. 2012; 76:431–8. [PubMed: 22236865]
8. Tandon M, Vemula SV, Sharma A, Ahi YS, Mittal S, Bangari DS, et al. EphrinA1-EphA2 interaction-mediated apoptosis and FMS-like tyrosine kinase 3 receptor ligand-induced immunotherapy inhibit tumor growth in a breast cancer mouse model. J Gene Med. 2012; 14:77–89. [PubMed: 22228563]
9. Yang NY, Fernandez C, Richter M, Xiao Z, Valencia F, Tice DA, et al. Crosstalk of the EphA2 receptor with a serine/threonine phosphatase suppresses the Akt-mTORC1 pathway in cancer cells. Cell Signal. 2011; 23:201–12. [PubMed: 20837138]
10. Noblitt LW, Bangari DS, Shukla S, Knapp DW, Mohammed S, Kinch MS, et al. Decreased tumorigenic potential of EphA2-overexpressing breast cancer cells following treatment with adenoviral vectors that express EphrinA1. Cancer Gene Ther. 2004; 11:757–66. [PubMed: 15359289]
11. Noblitt LW, Bangari DS, Shukla S, Mohammed S, Mittal SK. Immuno-competent mouse model of breast cancer for preclinical testing of EphA2-targeted therapy. Cancer Gene Ther. 2005; 12:46–53. [PubMed: 15486559]
12. Wang H, Wen J, Wang H, Guo Q, Shi S, Shi Q, et al. Loss of expression of EphB1 protein in serous carcinoma of ovary associated with metastasis and poor survival. Int J Clin Exp Pathol. 2014; 7:313–21. [PubMed: 24427352]
13. Wang JD, Dong YC, Sheng Z, Ma HH, Li GL, Wang XL, et al. Loss of expression of EphB1 protein in gastric carcinoma associated with invasion and metastasis. Oncology. 2007; 73:238–45. [PubMed: 18424888]
14. Guan M, Xu C, Zhang F, Ye C. Aberrant methylation of EphA7 in human prostate cancer and its relation to clinicopathologic features. Int J Cancer. 2009; 124:88–94. [PubMed: 18821581]
15. Oba SM, Wang YJ, Song JP, Li ZY, Kobayashi K, Tsugane S, et al. Genomic structure and loss of heterozygosity of EPHB2 in colorectal cancer. Cancer Lett. 2001; 164:97–104. [PubMed: 11166921]

16. Pasquale EB. Eph receptors and ephrins in cancer: bidirectional signalling and beyond. Nat Rev Cancer. 2010; 10:165–80. [PubMed: 20179713]
17. Alazzouzi H, Davalos V, Kokko A, Domingo E, Woerner SM, Wilson AJ, et al. Mechanisms of inactivation of the receptor tyrosine kinase EPHB2 in colorectal tumors. Cancer Res. 2005; 65:10170–3. [PubMed: 16288001]
18. Fox BP, Kandpal RP. Transcriptional silencing of EphB6 receptor tyrosine kinase in invasive breast carcinoma cells and detection of methylated promoter by methylation specific PCR. Biochem Biophys Res Commun. 2006; 340:268–76. [PubMed: 16364251]
19. Jin W, Qi S, Luo H. The effect of conditional EFNB1 deletion in the T-cell compartment on T-cell development and function. BMC Immunol. 2011; 12:68. [PubMed: 22182253]
20. Kuang SQ, Bai H, Fang ZH, Lopez G, Yang H, Tong W, et al. Aberrant DNA methylation and epigenetic inactivation of Eph receptor tyrosine kinases and ephrin ligands in acute lymphoblastic leukemia. Blood. 2010; 115:2412–9. [PubMed: 20061560]
21. Dokter WH, Tuyt L, Sierdsema SJ, Esselink MT, Vellenga E. The spontaneous expression of interleukin-1 beta and interleukin-6 is associated with spontaneous expression of AP-1 and NF-kappa B transcription factor in acute myeloblastic leukemia cells. Leukemia. 1995; 9:425–32. [PubMed: 7885041]
22. Kampen KR, Ter Elst A, Mahmud H, Scherpen FJ, Diks SH, Peppelen-bosch MP, et al. Insights in dynamic kinome reprogramming as a consequence of MEK inhibition in MLL-rearranged AML. Leukemia. 2014; 28:589–99. [PubMed: 24240200]
23. de Jonge HJ, Valk PJ, Veeger NJ, Ter Elst A, den Boer ML, Cloos J, et al. High VEGFC expression is associated with unique gene expression profiles and predicts adverse prognosis in pediatric and adult acute myeloid leukemia. Blood. 2010; 116:1747–54. [PubMed: 20522712]
24. Ross ME, Mahfouz R, Onciu M, Liu HC, Zhou X, Song G, et al. Gene expression profiling of pediatric acute myelogenous leukemia. Blood. 2004; 104:3679–87. [PubMed: 15226186]
25. Ter Elst A, Diks SH, Kampen KR, Hoogerbrugge PM, Ruijtenbeek R, Boender PJ, et al. Identification of new possible targets for leukemia treatment by kinase activity profiling. Leuk Lymphoma. 2011; 52:122–30. [PubMed: 21133721]
26. Noren NK, Foos G, Hauser CA, Pasquale EB. The EphB4 receptor suppresses breast cancer cell tumorigenicity through an Abl–Crk pathway. Nat Cell Biol. 2006; 8:815–25. [PubMed: 16862147]
27. Satyanarayana A, Hilton MB, Kaldis P. p21 Inhibits Cdk1 in the absence of Cdk2 to maintain the G1/S phase DNA damage checkpoint. Mol Biol Cell. 2008; 19:65–77. [PubMed: 17942597]
28. Boehrer S, Ades L, Tajeddine N, Hofmann WK, Kriener S, Bug G, et al. Suppression of the DNA damage response in acute myeloid leukemia versus myelodysplastic syndrome. Oncogene. 2009; 28:2205–18. [PubMed: 19398952]
29. Lord CJ, Ashworth A. The DNA damage response and cancer therapy. Nature. 2012; 481:287–94. [PubMed: 22258607]
30. Lindquist R, Forsblom AM, Ost A, Gahrton G. Mutagen exposures and chromosome 3 aberrations in acute myelocytic leukemia. Leukemia. 2000; 14:112–8. [PubMed: 10637485]
31. Tchinda J, Dijkhuizen T, Vlies PP, Kok K, Horst J. Translocations involving 6p22 in acute myeloid leukaemia at relapse: breakpoint characterization using microarray-based comparative genomic hybridization. Br J Haematol. 2004; 126:495–500. [PubMed: 15287941]
32. Fasen K, Cerretti DP, Huynh-Do U. Ligand binding induces Cbl-dependent EphB1 receptor degradation through the lysosomal pathway. Traffic. 2008; 9:251–66. [PubMed: 18034775]
33. Coenen EA, Driessen EM, Zwaan CM, Stary J, Baruchel A, de Haas V, et al. CBL mutations do not frequently occur in paediatric acute myeloid leukaemia. Br J Haematol. 2012; 159:577–84. [PubMed: 23025505]
34. Teng L, Nakada M, Furuyama N, Sabit H, Furuta T, Hayashi Y, et al. Ligand-dependent EphB1 signaling suppresses glioma invasion and correlates with patient survival. Neuro Oncol. 2013; 15:1710–20. [PubMed: 24121831]
35. Huang WY, Hsu SD, Huang HY, Sun YM, Chou CH, Weng SL, et al. MethHC: a database of DNA methylation and gene expression in human cancer. Nucleic Acids Res. 2015; 43:D856–61. [PubMed: 25398901]

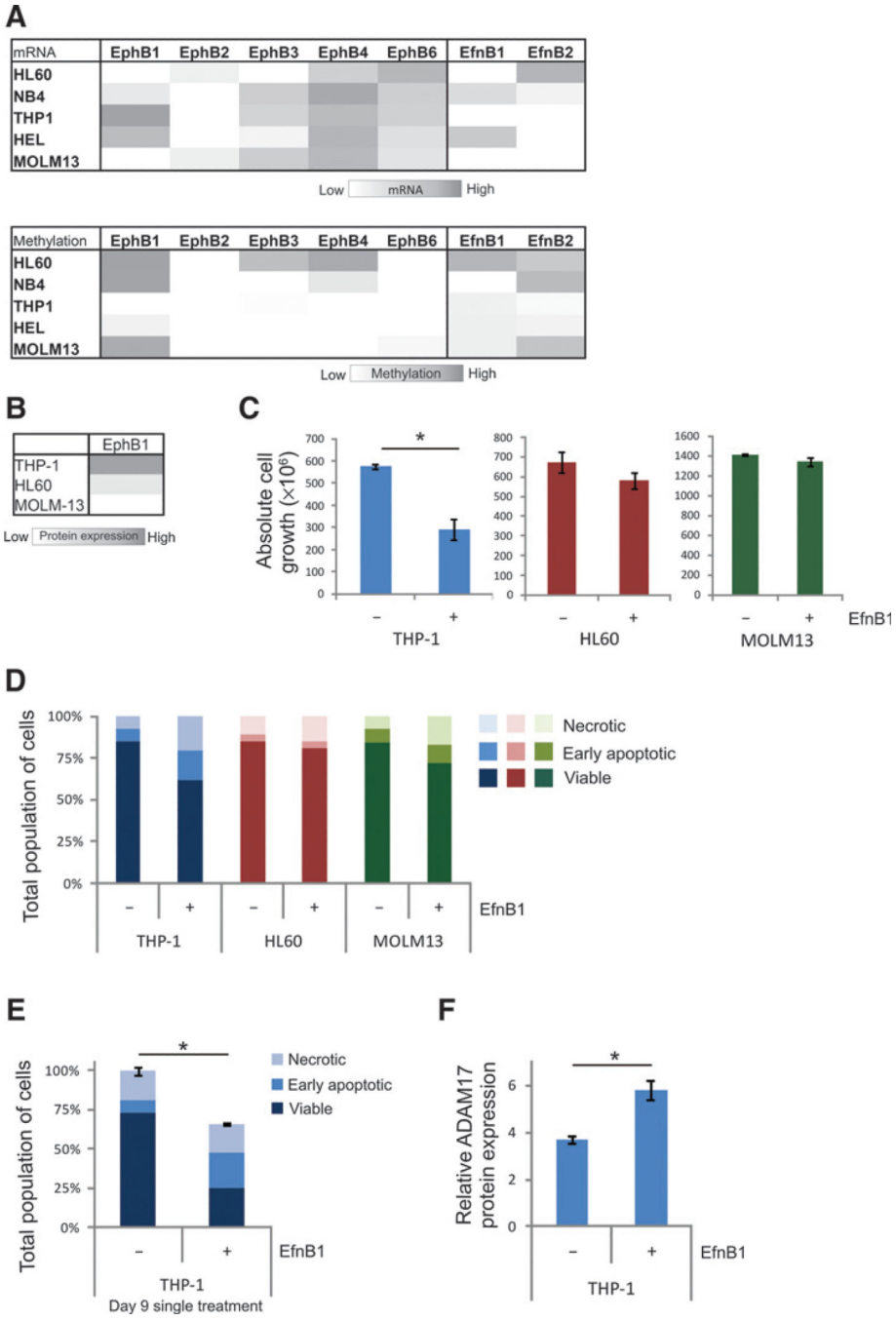

Figure 1.

A role for *EphB1* suppression in AML; EfnB1 ligand mediated reduction of proliferation and induced apoptosis of AML cells. A, a heatmap of the mRNA expression levels and methylation density of EphB receptors and EfnB ligands in five AML cell lines, measured using quantitative RT-PCR analysis and bisulfite pyrosequencing. B, a heatmap of flow cytometric EphB1 membrane protein expression levels in AML cell lines (range, 10%–70% of AML cell line population with EphB1 expression). C, growth analysis by absolute cell counts after 72 hours incubation with EfnB1 in AML cell lines in three independent

experiments (mean ± SEM; *, $P = 0.001$). D, flow cytometric apoptosis analysis was performed by annexin V/PI staining of 72 hours EfnB1-stimulated and -untreated AML cell lines. E, cell survival analysis at day 9 by a single dose of EfnB1 treatment in THP-1 (mean ± SEM, $P = 0.022$). F, ADAM17 expression measured using ELISA of untreated and EfnB1 treated AML cell lysates after 24 hours of treatment (mean ± SEM, $P = 0.015$).

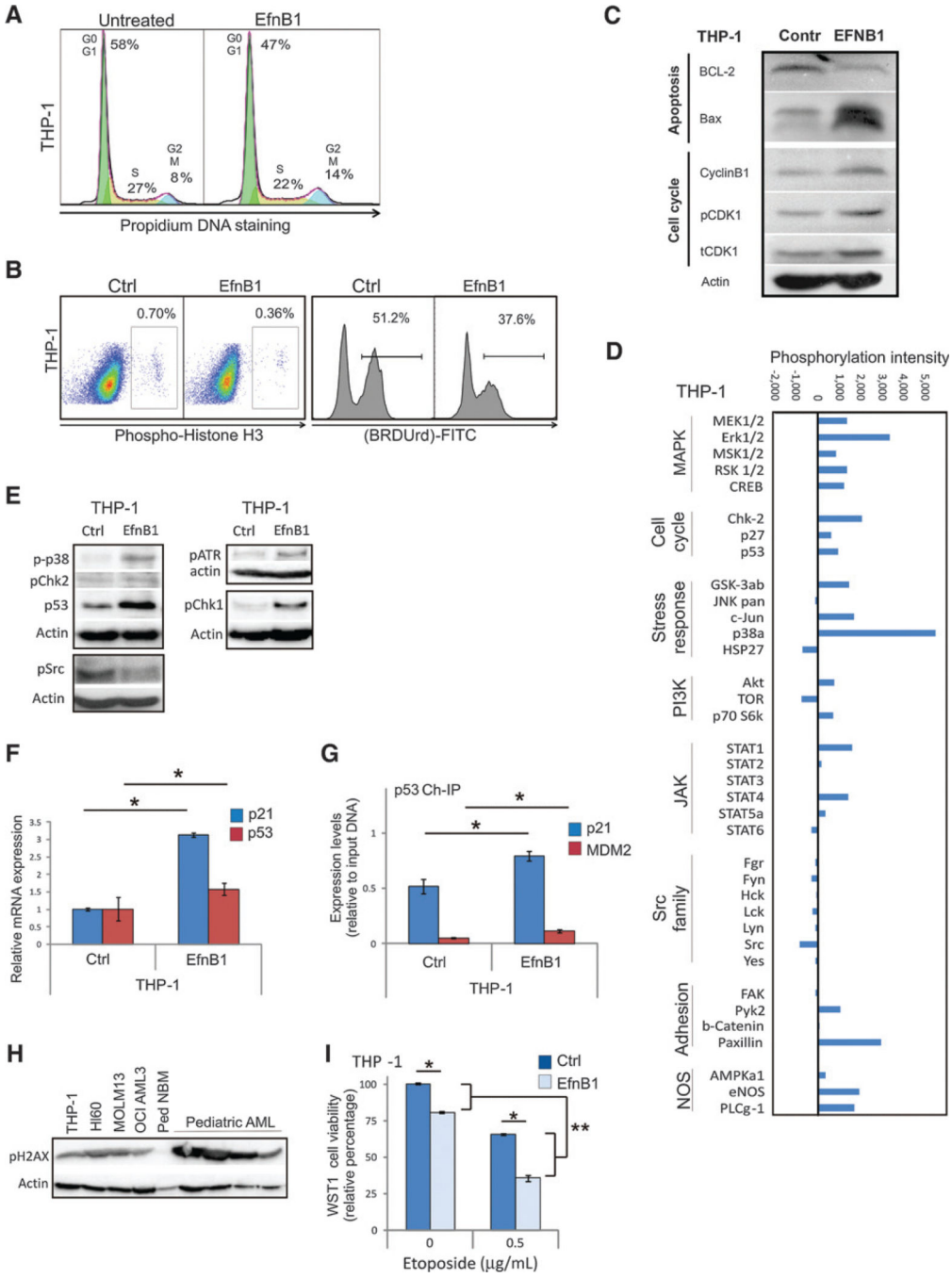

Figure 2.

EfnB1 induced G_2–M cell-cycle arrest is causative for the reduced proliferation and the increased apoptosis in EphB1^{high} THP-1 AML cells. A, flow cytometric analysis of cell-cycle compartments by PI DNA staining of viable THP-1 cells either untreated of EfnB1 treated for 24 hours. B, flow cytometric analysis of phospho-histone H3 mitotic spindle staining of THP-1 cells either untreated or EfnB1 treated for 24 hours; flow cytometric BRDU incorporation analysis after 48 h EfnB1 treatment. C, immunoblot analysis of apoptosis and cell-cycle regulating proteins; Bcl-2, Bax, CyclinB1, phospho-CDK1^{tyr15},

CDK1, and actin showing the effect of 72 hours EfnB1 stimulation of THP-1 cells versus untreated control cells. D, phosphoproteomic analysis of 72 hours EfnB1-stimulated THP-1 cells versus untreated control cells. This bar graph displays the absolute changes in protein kinase phosphorylation upon EfnB1 stimulation of THP-1 cells. E, immunoblot analysis of ATR, Chk1, Chk2, p53, p38, and Src phosphorylation in EfnB1-stimulated cells versus untreated THP-1 cells. F, Quantitative RT-PCR analysis of *p21* and *p53* in 24 h EfnB1-stimulated THP-1 cells versus untreated control cells, confirming the phoshoproteome analysis (mean ± SEM, *, $P < 0.001$). G, ChIP analysis of p53 in EfnB1-treated THP-1 cells (20 hours) as compared with untreated controls. Quantitative RT-PCR for *p21* and *MDM2* was performed to determine p53 DNA-binding capacity (mean ± SEM; *, $P < 0.001$). H, DNA damage defined by phospho-yH2AX expression by immunoblot analysis of AML cell lines, pediatric NBM control samples, and pediatric AML patient samples. I, etoposide induced AML genotoxicity effects on the AML cell survival in untreated and EfnB1-treated THP-1 cells upon 48 hours treatment, as measured by WST-1 cell survival assay (mean ± SEM); *, significant difference between experimental groups; **, significant additive effects between experimental groups.

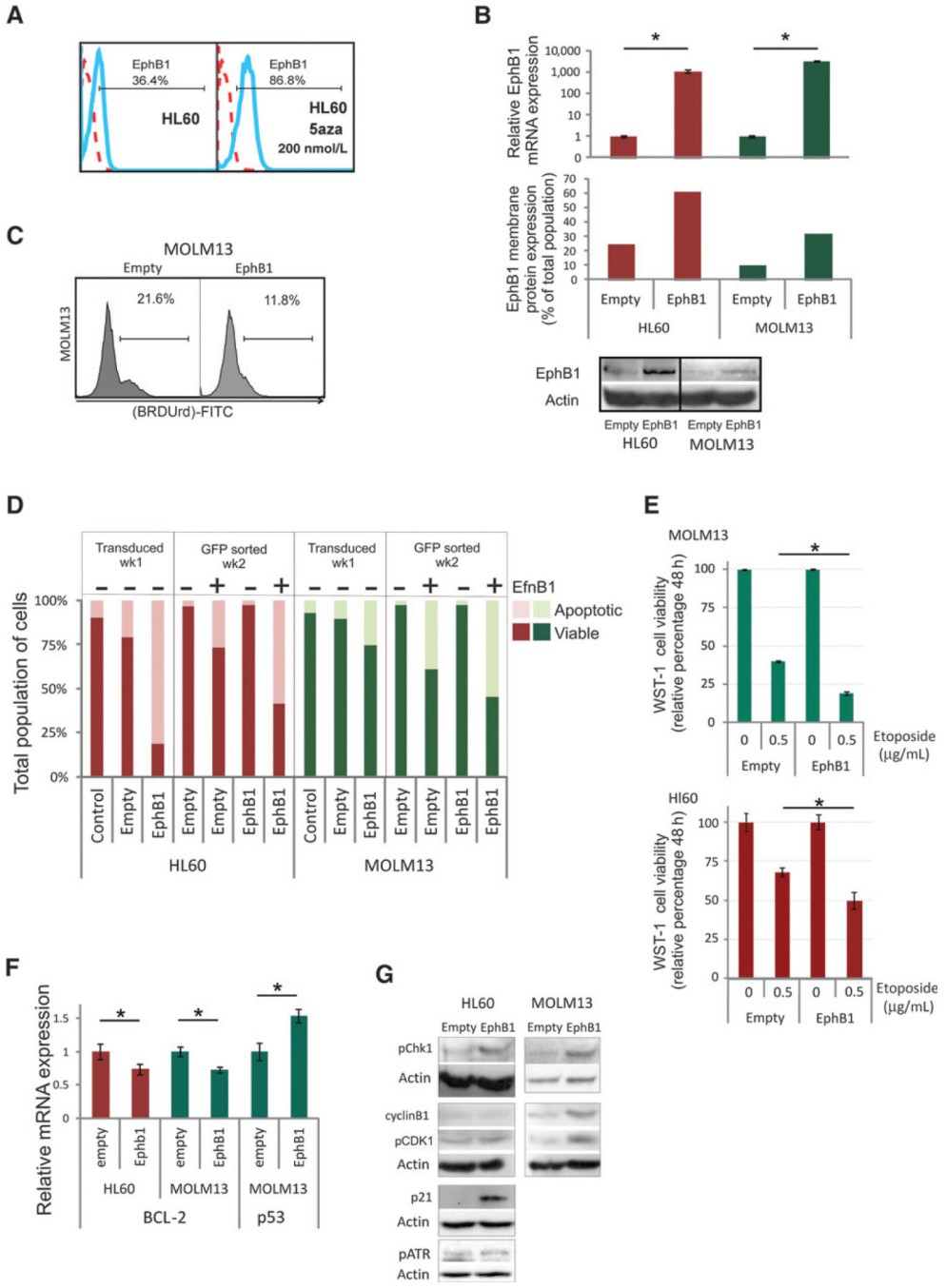

Figure 3.

EphB1 overexpression severely induced apoptosis in *EphB1*-methylated AML cell lines. A, EphB1 membrane protein expression analysis by flow cytometry after 24 hours 5-Aza-2′-deoxycytidine treatment of *EphB1*-methylated HL60 AML cells. B, quantitative RT-PCR analysis of *EphB1* mRNA expression to confirm the *EphB1* overexpression in GFP-expressing cells (mean ± SEM; *, $P < 0.001$). Flow cytometric analysis showed that the increased*EphB1* mRNA expression could be translated into induced EphB1 membrane protein expression in both HL60 and MOLM-13 cells *EphB1* tranduced cells. To confirm the

induction in EphB1 protein expression, we simultaneously performed immunoblot analysis of EphB1, demonstrating that indeed *EphB1*-tranduced cells express higher levels of EphB1 protein. C, flow cytometric apoptosis analysis is performed by annexin V-PE staining of 72 hours EfnB1-treated and -untreated transduced HL60 and MOLM13 cells comparing empty vector controls with *EphB1*-overexpressing cells. D, BrdUrd incorporation analysis for cell proliferation in MOLM13 empty vector controls and EphB1 overexpression cells. E, etoposide induced AML genotoxicity effects on the AML cell survival in untreated and EfnB1-treated MOLM13 transduced cells upon 48 hours treatment, as measured by WST-1 cell survival assay (mean ± SEM). F, quantitative RT-PCR analysis of *Bcl-2* and *p53* comparing EfnB1-treated empty vector control and *EphB1*-overexpressing HL60 and MOLM13 cells (mean ± SEM; *, $P < 0.05$). G, immunoblot analysis of pChk1, Cyclin B1, pCDK1 (Tyr15), p21, pATR protein expression in empty vector controls, and EphB1-overexpressing HL60 and MOLM13 cells; *, significant difference between experimental groups.

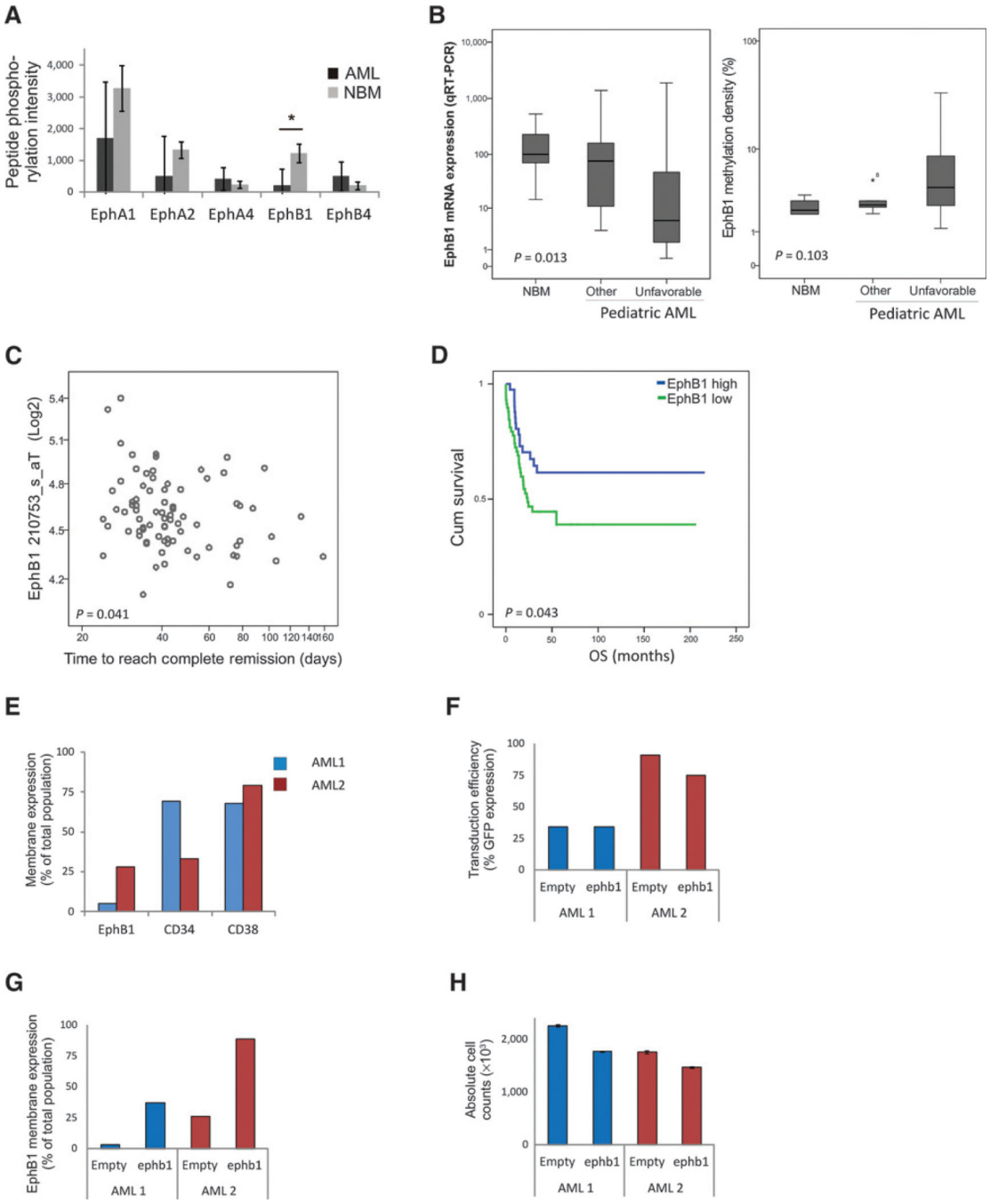

Figure 4.

EphB1 suppression in primary pediatric AML. A, bar graph of Ephrin receptor peptide activity in pediatric AML ($n = 6$) and NBM ($n = 5$) lysates (mean ± SEM; *, $P = 0.022$). B, the left box-plot presenting the mean *EphB1* mRNA expression levels as determined using quantitative RT-PCR in NBM controls ($n = 8$), other pediatric AML samples ($n = 9$, NK, INV(16), t(8;21), insertion 8, −9q)), and unfavorable AML pediatric patient samples ($n = 18$, complex and 11q23; mean ± SEM, $p = 0.013$). The right box-plot shows the *EphB1* methylation density in NBM controls ($n = 4$), other pediatric AML samples ($n = 11$), and

unfavorable AML pediatric patients samples ($n = 10$; mean ± SEM, $p = 0.103$). C, *EphB1* mRNA expression correlated with the time to reach a complete remission using gene-expression array analysis of a large pediatric AML cohort ($n = 79$, $P = 0.041$). D, cumulative survival curve comparing pediatric AML patient samples with high *EphB1* expression versus samples with low *EphB1* expression (with the mean as threshold, high EphB1 expression $n = 42$ and low expression $n = 58$, $P = 0.043$). E, bar graph of EphB1, CD34, and CD38 expression levels in two independent AML patients' samples determined by flow cytometry. F, flow cytometric analysis of transduction efficiencies after stable introduction of a constitutive *EphB1* overexpression vector in two independent pediatric AML samples. G, EphB1 membrane protein overexpression levels in empty vector and *EphB1* overexpression pediatric AML samples using flow cytometric analysis. H, this bar graph presents the absolute cell counts 7 days after transduction of two primary pediatric AML samples comparing empty vector controls with *EphB1* overexpression vectors (mean ± SEM).